



# The impact of wind power growth and hydrological uncertainty on financial losses from oversupply events in hydropower-dominated systems



Yufei Su<sup>a,\*</sup>, Jordan D. Kern<sup>b</sup>, Gregory W. Characklis<sup>a</sup>

<sup>a</sup> Department of Environmental Science and Engineering, Rosenau Hall, CB# 006, University of North Carolina at Chapel Hill, Chapel Hill, NC 277517, United States

<sup>b</sup> Institute for the Environment, University of North Carolina at Chapel Hill, United States

## HIGHLIGHTS

- Oversupply can lead to financial losses when renewable energy is curtailed.
- Oversupply losses will increase as a function of installed wind capacity.
- Adding transmission capacity is not a cost effective solution to oversupply.

## ARTICLE INFO

### Article history:

Received 11 November 2016

Received in revised form 8 February 2017

Accepted 22 February 2017

Available online 11 March 2017

### Keywords:

Oversupply

Renewable energy

Financial risk

Present value loss

## ABSTRACT

The rapid expansion of variable renewable energy (e.g., wind and solar) can make it more difficult to balance electricity supply and demand at a grid-scale. While much attention has focused on the risk of unexpected generation shortfalls, periods of oversupply (when supply is greater than demand) also present challenges that can lead to financial losses for utilities and/or consumers when renewable energy is “curtailed”. A unique form of oversupply occurs in hydro-dominated systems. Although hydropower is thought to offer a highly flexible resource that can complement variable renewable energy, seasonal variability in streamflows and the presence of environmental regulations can create complex oversupply conditions if renewable energy is plentiful. In this study, an integrated hydro-economic model is developed to assess the frequency and severity of financial losses arising from oversupply in the U.S. Pacific Northwest, a hydro-dominated system with rapidly growing wind power generation. Present value losses over 25 years (2016–2040) are evaluated under several future scenarios including increased wind capacity, electricity price uncertainty, and expanded transmission capacity for moving excess electricity to export markets. Results indicate that oversupply losses will increase as a function of installed wind capacity, with the extent of this increase sensitive to future electricity prices. In the case of adding transmission capacity to alleviate oversupply losses, the cost of this infrastructure is substantially more than the associated reduction in losses and is therefore difficult to justify.

© 2017 Elsevier Ltd. All rights reserved.

## 1. Introduction

Wind power capacity worldwide is increasing at a rapid rate, with installed global capacity having increased roughly 2400% from 2000 to 2015 [1]. Nonetheless, an ongoing challenge with increasing wind capacity is managing wind power’s variability [2,3]. Wind speeds can change dramatically on multiple time scales, and existing power systems sometimes struggle to accommodate these sudden changes [4,5]. One challenge associated with

the variability of wind is generation “oversupply”. Oversupply occurs when the total electricity generation in a region exceeds internal demand [6,7]. In general, generation oversupply happens due to the presence of some combination of “must run” thermal generation (e.g., nuclear) and hydropower that cannot be turned off or sufficiently ramped down, and variable renewable energy.

During oversupply events, excess electricity that cannot be exported to another region or stored via batteries or pumped storage [8] must be curtailed in order to maintain the integrity of the electricity grid. Often, renewables like wind and solar power are curtailed because it is the most economically and/or viable way to balance load and generation [6,9]. Without significant improvements in transmission capacity, energy storage, and demand side

\* Corresponding author.

E-mail address: [yufeisu@live.unc.edu](mailto:yufeisu@live.unc.edu) (Y. Su).

management, oversupply is likely to become a greater challenge in the future as wind and solar capacity increases [7–12].

Many studies have addressed the issue of renewable energy curtailment from an economic perspective. Some point out that it wastes energy, leading to economic losses for both utilities and society [11,13,14]. Others, however, have concluded that, given the cost of transmission and energy storage options, renewable energy curtailment may be a socially optimal choice [10]. The range of conclusions drawn from previous studies suggests that oversupply problems in different systems can be very distinct. The financial losses associated with curtailment may depend on a number of factors, including complex interactions between different types of generation, the price of electricity in deregulated markets, as well as climatic and environmental factors, making for challenges in both characterizing the problem and solving it.

Power systems in Germany and China, as well as regional energy systems in the U.S. (e.g., PJM Interconnection and ERCOT (Electric Reliability Council of Texas) and MISO (Midcontinent Independent System Operator)) have experienced generation oversupply due to the combination of must run thermal generation and greater renewable capacity, in particular wind power [8,9,15]. Another form of generation oversupply can occur in hydropower-dominated systems, especially in situations where high levels of renewables are present [9]. Hydropower, due to its operational flexibility, is often regarded as an ideal resource to compensate for the intermittency and unpredictability of wind power [16,17]. However, as more wind penetrates the electricity mix, hydroelectric dams may be limited in their ability to dramatically reduce generation to accommodate increase in wind power, especially if the operations of dams are constrained by multi-purpose obligations or environmental regulations.

Oversupply problems in hydropower-dominated systems are unique because they are a product of both hydrological variability and wind variability. Study of this issue has been limited, however, partly because accurately characterizing the frequency and severity of oversupply losses requires a modeling approach that integrates both the complexity of the reservoir system (accounting for both watershed hydrology and dam operating rules) and the larger power system (including alternative thermal sources, variable load and renewable production as well as transmission constraints). In order to facilitate exploration of oversupply problems in hydropower-dominated systems, a transferrable methodological approach is needed.

The goal of this study is to develop an integrated modeling framework that couples multi-scale stochastic time series modeling with a mass-balance reservoir network model to facilitate a probabilistic assessment of financial losses from oversupply. This integrated modeling framework is then applied to a hydropower-dominated system in the U.S., the Bonneville Power Administration control area. Losses from oversupply are quantified over an ensemble of 25-year trajectories (2016–2040), and the sensitivity of oversupply losses to various factors is explored, including: (1) the rate of wind capacity growth; (2) investment in additional export transmission capacity; and (3) fluctuations in wholesale electricity prices. The results of this work provide an improved understanding of the key factors driving financial losses from oversupply in hydropower-dominated systems. They also inform the development of better system planning strategies that accurately value the economic benefits of oversupply mitigation strategies (i.e., construction of additional export transmission capacity).

## 2. Methods

A primary goal of this study is to gain a probabilistic understanding of financial losses caused by oversupply events in

hydropower-dominated systems. To do so, the following approach is taken. First, the study area of interest is chosen. Then an integrated modeling framework is developed, and its ability to replicate observed instances of oversupply and accurately estimate associated financial losses is validated. A sensitivity analysis is performed in order to understand the relative impacts of wind capacity growth and electricity prices on oversupply losses. Finally, present value losses are evaluated over an ensemble of 25-year trajectories (2016–2040) assuming gradual growth in wind capacity, and the question of whether investment in additional transmission capacity represents an economically viable mitigation strategy is answered.

It should be noted that “financial losses” discussed in this work differ from “economic losses”. We define financial losses simply as the monetary value of curtailed wind power production. This value does not include the broader economic losses that may include impacts to other system participants (i.e., customers in adjacent systems) or potential externalities.

### 2.1. Study area

Perhaps the most prominent example of oversupply in hydropower-dominated systems is the U.S. Pacific Northwest, where hydropower meets more than 60% of regional electricity demand [18]. Most of the Pacific Northwest’s electric power system is operated by Bonneville Power Administration (BPA), a federal power marketing organization that is in charge of power plant operations, transmission, and grid balancing [18]. Within BPA’s footprint there are 31 federal hydroelectric dams and many additional non-federal dams, 1 federal nuclear plant and other non-federal thermal plants [18]. This system has experienced rapid growth in wind power capacity and is already experiencing oversupply issues, with two major wind related oversupply events occurring in 2011 and 2012. Thus, BPA is a logical choice for the application of the proposed modeling framework.

Oversupply events in the BPA system occur as a result of a complex interaction between snowmelt-driven hydrology, wind power availability, limited export transmission capacity, and environmental regulations on the operation of hydroelectric dams (see Fig. 1). During periods of high streamflow (peak summer snowmelt), hydroelectric dams in BPA’s system, including many found in the Federal Columbia River Power System (FCRPS), a network of hydroelectric dams spanning several states, produce massive amounts of hydropower. In response, thermal power plants are shut down or ramped down to their operational limits [19–21] in order to maximize the use of hydropower. Nonetheless, with wind power capacity in the region growing quickly, the combination of summer hydropower production and wind power can create periods of system-wide generation oversupply. With limited transmission capacity for exporting excess electricity to other systems (i.e., California and British Columbia), resolving oversupply issues in the BPA system is a challenge that ultimately falls to generators within the system.

As a first recourse, dams reduce hydropower production (thereby maximizing the use of wind power) and store water for release at a later time. Ultimately, however, storing inflows drives reservoir levels higher and exhausts the ability of dam operators to store any additional water. The next recourse available to dam operators is to “spill” water (i.e., discharge it from reservoirs without generating electricity). In the FCRPS, however, environmental regulations on flows downstream of some hydroelectric dams limit the dams’ ability to spill water in order to accommodate high wind energy penetration. Specifically, spilling large volumes of water can cause elevated downstream levels of total dissolved gases [22], a violation of federal water quality standards. Thus, the combination of high reservoir levels and water quality regulations can,

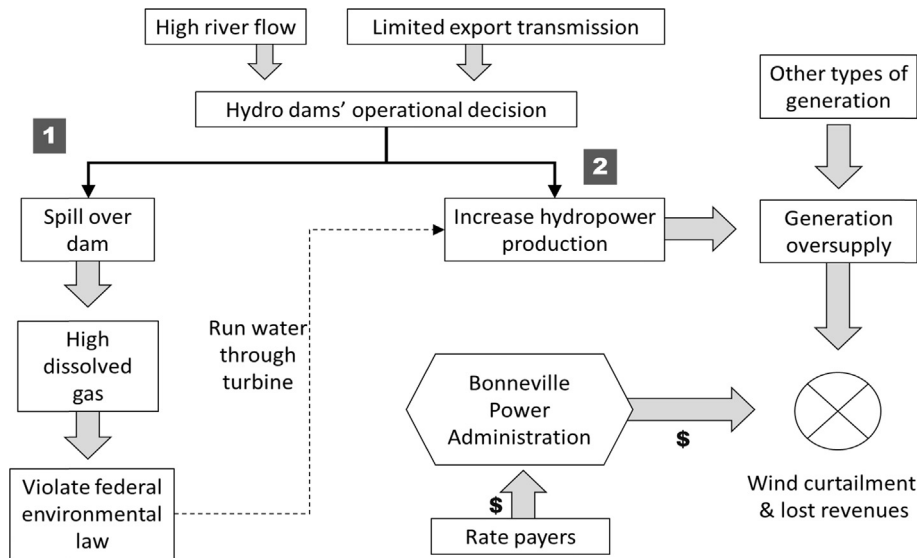


**Fig. 1.** A schematic view of oversupply events faced by BPA. During high flow periods, hydropower producers have two options. Option 1 is spilling more water, which will lead to the violation of federal law. In Option 2, water is instead passed through turbines, which generates excess electricity and leads to oversupply.

by limiting spilling, effectively turn dams in the FCRPS into “must run” resources that have no choice but to generate electricity.

As a result, during oversupply events, it is often wind producers in the region who are ordered to shut down in order to maintain a system-wide balance between supply and demand. Wind power curtailment results in the loss of revenues from wind power generation, which includes the loss of associated renewable energy credits and production tax credits. Since 2012, wind producers have been compensated by BPA for all oversupply losses, and this bill is ultimately passed to rate payers [23].

The financial losses caused by these recent oversupply events in BPA’s system (as well as discussion of strategies for mitigating future losses) have drawn significant media attention [24]. Wind power capacity in this region is expected to grow dramatically in coming decades, potentially leading to more severe financial consequences from oversupply. Installed wind capacity increased from almost nothing in the year 2000–4782 MW by the end of 2014. An additional 3000–4000 MW of wind power capacity is projected to be installed by the end of 2025 [25].

BPA has suggested that annual losses moving forward could be as much as \$50 million U.S. dollars [24]. However, in a preliminary analysis BPA conducted on potential oversupply losses, only four non-consecutive sample years from the historical hydrological record were considered, neglecting large swaths of the distribution of potential hydrological events and making no effort to project losses over longer representative time frames. In addition, BPA’s preliminary analysis also assumed static or very limited changes in installed wind capacity, transmission availability and electricity prices over time. Given the projected rapid growth of wind power in the system, and the uncertainty with respect to these other factors, a more comprehensive approach is desired to understand how the challenge of managing oversupply in hydropower-dominated systems like BPA’s may evolve in the future, and how transmission planning and electricity price behavior may contribute to either lessening or worsening the problem.

## 2.2. Data sources

As a federal power market administration whose system is well established and monitored, BPA has large amounts of publicly available operating data. This study makes use of eight years (from 2007 to 2014) of hourly system-wide wind power production, elec-

tricity demand, transmission export and thermal generation data that are available from BPA [18]. Inflow data at hydroelectric dams in the FCRPS were obtained from BPA’s modified flow dataset [26]. This dataset provides 80 years of river flow data (from 1928 to 2008) that account for factors such as withdrawals and return flows from irrigation, evaporation and other water consumption in the region. Eighty years of daily temperature data, from 1928 to 2008, were obtained from the National Oceanic and Atmospheric Administration [27].

## 2.3. Integrated modeling framework and scenario development

The integrated modeling framework developed in this study is composed of several connected modules shown in Fig. 2. Exogenous drivers of the model include unregulated streamflow (i.e., inflows at reservoirs that have not been routed by an upstream dam), electricity demand, wind energy production, and transmission exports. These processes are represented via stochastic time series generation, and the resultant synthetic data products then serve as inputs to the power system “decision making” process, which includes the daily reservoir operations and hourly power scheduling modules. The output of the hourly power scheduling module is then processed to assess financial losses from oversupply.

### 2.3.1. Synthetic unregulated streamflow generation

Since excess hydropower production during high flow periods is a primary driver of oversupply events in hydropower-dominated systems, estimates of associated financial losses should be based on as large a sample of hydrological data as possible, and (ideally) include the potential for years in the future to look different than years experienced in the past. In many systems, this recommends use of an expanded, synthetic hydrological dataset.

Two main challenges exist in synthesizing streamflow data for use in reservoir network models. First, the synthesized streamflow has to be able to replicate statistical characteristics of the historical record. Second, the method must be able to generate values that demonstrate accurate spatial cross-correlations, as well as temporal autocorrelations. This study makes use of a K-nearest neighbor (K-NN) resampling method developed by Nowak et al. [28] that sufficiently addresses both requirements while generating synthetic daily flows for multiple, spatially distributed sites. This

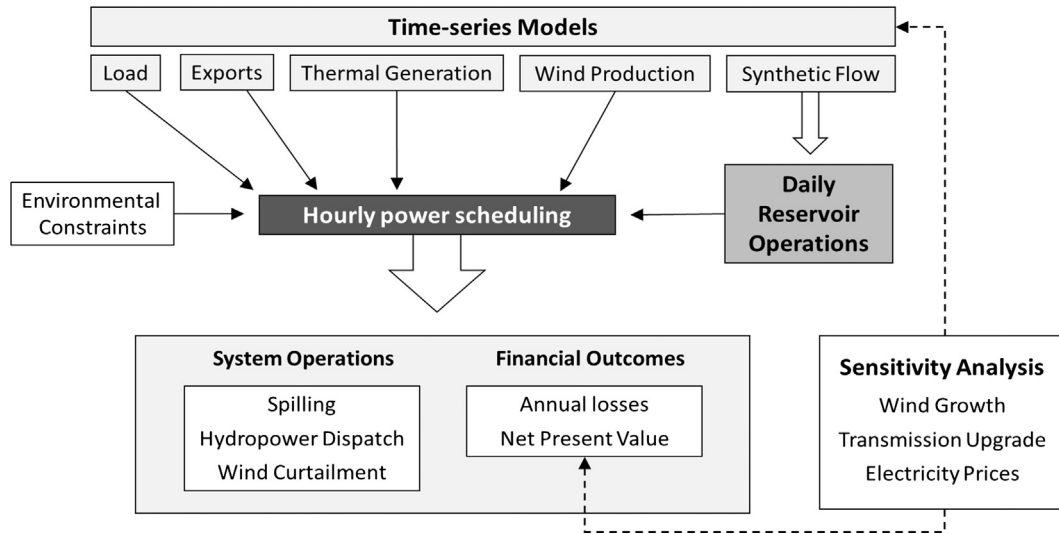


**Fig. 2.** Model integration overview. Load, system exports, thermal generation and wind generation are modelled as time series. Synthetic stream flow act as an input to the daily reservoir operations model, which calculates available hydropower production. This information is then sent to the hourly power scheduling model to determine spilling and wind curtailment.

approach entails use of a lag-1 auto-regressive (AR) model to simulate total annual flows, and combines these annual values with vectors of daily flow fractions, which are conditionally resampled from the historical record. The results of this synthetic streamflow generation process are daily time-series of unregulated flows throughout the reservoir network that replicate key elements of the historical distribution while also providing for the possibility of daily streamflows that are lower/higher than any previously observed value. A detailed explanation of this technique can be found in the [Supplemental Information section](#).

### 2.3.2. Air temperature modeling

Electricity demand is heavily influenced by activities that heat and cool buildings [29], so daily mean air temperatures are used as a primary input in simulating electricity demand. Air temperatures can also have direct effects on the timing of snowmelt, which is the main source of stream flow in the BPA system. Thus, it is important to understand and account for any existing covariance structures between temperatures and streamflow patterns when generating both synthetic streamflow and temperature data. To account for this relationship, when years of flow fractions are conditionally resampled from the historical record, daily mean temperatures are simultaneously resampled from the same year. This process ensures the sufficient capture of covariance between temperature and streamflow (from snowmelt) in terms of magnitude and timing.

As one of the dominant drivers of electricity demand, daily air temperature features prominently in most commonly used approaches for simulating daily peak electricity demand [2,28]. In this study, the population weighted mean daily temperature is used to capture the temperature effect on daily peak demand across BPA’s control area. Population and temperature data are taken from the most populated city in each of the primary states in BPA’s footprint, namely Seattle, WA, Portland, OR, and Boise, ID. The population weighted temperature is calculated as:

$$Tw_i = \sum_{i=1}^3 \frac{P_i}{\sum_i P_i} T_i \quad (1)$$

where

$Tw_i$  = Population weighted temperature  
 $i$  = index for 3 different cities

$P_i$  = Population in the indexed city  
 $T_i$  = Mean daily temperature in the indexed city.

### 2.3.3. Hourly electricity demand modeling

The method used here to model hourly electricity demand combines empirically derived hourly demand profiles for each day of the year formed from historical data, with a synthetic record of peak daily electricity demand.

First, hourly demand profiles are extracted from historical electricity demand data for the relevant system (in this case, BPA). Hourly demand profiles for each calendar day are created in a  $(24 \times 365)$  matrix  $S$ , with elements equal to:

$$S_{h,d} = E \left[ \frac{L_{h,d}}{L'_{h,d}} \right] \quad (2)$$

where

$L_{h,d}$  is the demand at hour  $h$  in calendar day  $d$   
 $L'_{h,d}$  is the maximum hourly demand in calendar day  $d$ .

Hourly demand profiles are then multiplied by a synthetic time series of daily peak electricity demand in order to simulate hourly demand. Given coincident time series of historical daily peak demand and population weighted temperature, a piecewise linear relationship is developed. This relationship is then removed from the daily peak demand data for whitening.

After removing temperature effects, the remaining peak demand process contains some residual non-temperature related month effects and day of the week effects. Month effects are removed by subtracting the monthly mean and dividing by the standard deviation for each month. Then day of the week effects are removed using a similar approach (Eq. (3)).

$$M = \frac{\left[ \left( \frac{L_d^* - \mu_{dm}}{\sigma_{dm}} \right) - \mu_{dow} \right]}{\sigma_{dow}} \quad (3)$$

where

$M$  = daily peak demand data, with effects from temperature, month and day of week removed (MW)  
 $L_d^*$  = load data with temperature effects removed  
 $\mu_{dm}$  = the expected demand of the month  $m$

$\sigma_{d_m}$  = the standard deviation of the month  $m$   
 $\mu_{dow}$  = the expected demand for day-of-the-week ( $dow$ )  
 $\sigma_{dow}$  = the standard deviation for day-of-the-week ( $dow$ ).

The remaining process,  $\mathbf{M}$  is fit to an Auto Regressive Moving Average (ARMA) model for simulation. The number of AR lags is selected based on the partial autocorrelation function, and the number of MA lags is selected by examining the autocorrelation function.

A synthetic time series of daily data ( $\mathbf{M}^*$ ) is simulated by the ARMA model for a desired duration, then the filtered signals are added back to the simulated result, now using a synthetic time series of population-weighted daily mean temperature.

$$L_{sim} = ((M^* \sigma_{dow} + \mu_{dow}) \sigma_{d_m}) + \mu_{d_m} + f(T^*) \quad (4)$$

where

$L_{sim}$  = simulated peak demand (MW) time series  
 $M^*$  = daily ARMA simulation  
 $f(T^*)$  = piecewise linear effects of temperature on peak demand  
 $T^*$  = synthetic population weighted daily mean temperature.

After generating  $L_{sim}$  (simulated daily peak demand data), it is applied to the hourly profiles for each calendar day taken from historical data (matrix  $\mathbf{S}$ ). Fig. 3 shows a validation of the electricity demand model. This model accurately preserves both daily and hourly autocorrelation and seasonality from the observed record. To reflect the gradual growth of electricity demand in the region over time under normal economic conditions, an annual growth rate of 0.9% is incorporated into the final time series [31].

### 2.3.4. Stochastic wind power modeling

A number of methods exist for modeling wind power production, with different methods able to excel under different conditions and study requirements [32–35]. This study uses a similar approach to the one conducted by Papavasili and Oren [35] that integrates representation of wind power production across four temporal scales: annual, seasonal, daily and hourly. Since a large driver of future oversupply events is expected to be increasing wind power capacity, this gradual increase of wind power capacity needs to be accounted for on an annual basis. Wind power generation can also demonstrate strong seasonality (in the BPA system

production tends to peak between mid-summer to early fall). On a daily basis, wind power generation demonstrates significant levels of autocorrelation as a result of memory in meteorological systems; and on an hourly level, wind power generation demonstrates a diurnal pattern (e.g., in the BPA system wind speeds and wind power production is higher during night and lower during the day). The approach used accurately reproduces observed statistical and time series properties of monthly, daily and hourly wind power production, while also providing an ability to scale wind power production to any theoretical amount of installed capacity.

First, the original dataset of hourly wind power production is log-transformed and then normalized by month and year as follows:

$$N\_Wind = \frac{\text{Log}_{Wind} - \text{Log}_{\mu_{m,y}}}{\text{Log}_{\sigma_{m,y}}} \quad (5)$$

where

$h$  = hour of the day  
 $m$  = month of the year  
 $y$  = sampling year  $\in \{2007, 2008, \dots, 2014\}$   
 $\text{Log}_{Wind}$  = log transformed hourly wind production  
 $\text{Log}_{\mu_{m,y}}$  = the mean of log transformed hourly wind production in month  $m$  and year  $y$   
 $\text{Log}_{\sigma_{m,y}}$  = standard deviation of log transformed wind production in month  $m$  and year  $y$ .

The above transformation generates the vector  $\mathbf{N\_Wind}$ , which is the hourly wind generation signal with monthly and annual (installed capacity effects) removed. We calculate daily mean values of  $\mathbf{N\_Wind}$  and then subtract these from each discrete 24-h period. This leaves a residual process,  $\mathbf{N\_Wind}'$ , that is a combination of autocorrelated hourly noise and diurnal signal. We then fit the calculated daily mean values to twelve separate ARMA models **Daily\_ARMA**, one for each calendar month.

Twelve diurnal signals (one for each calendar month) are then calculated as the mean value of  $\mathbf{N\_Wind}'$  data for each hour of the day:

$$Diurnal_{m,h} = E[N\_Wind'_{m,h}] \quad (6)$$

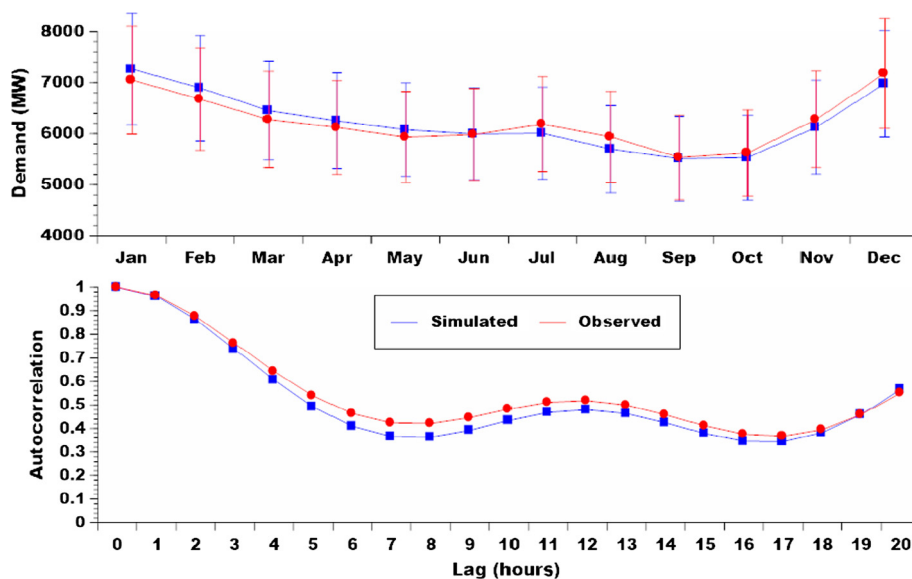


Fig. 3. Historical and simulated electricity hourly average demand in each month (upper panel) and autocorrelation (lower panel).

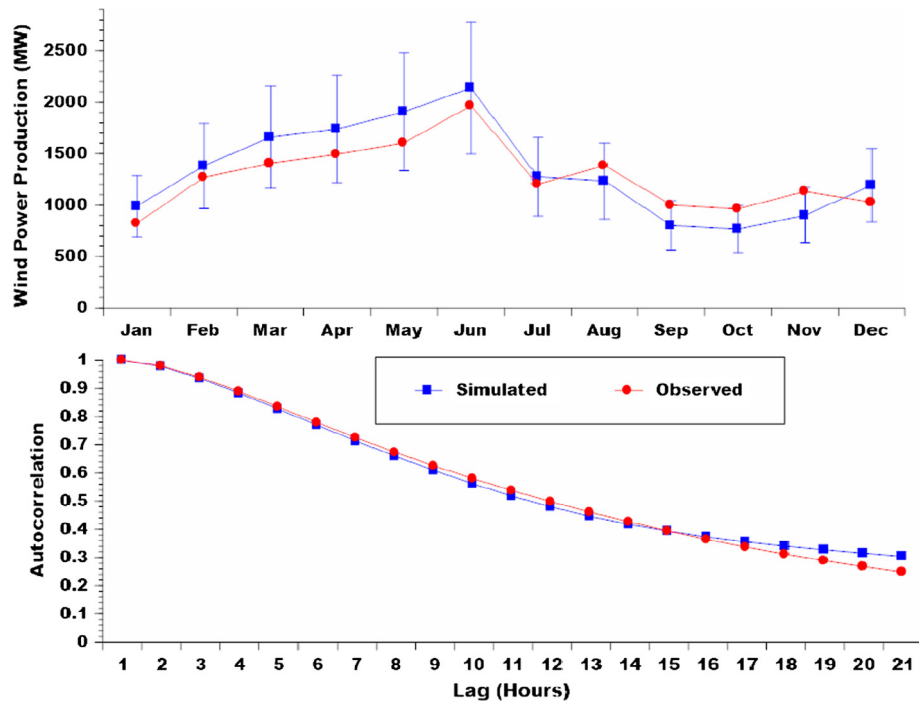


Fig. 4. Historical and simulated electricity demand (upper panel) and autocorrelation (lower panel).

These diurnal signals are then subtracted from the  $N\_Wind$  data, leaving an hourly zero-mean ARMA process, that describes the autocorrelated “noise” around the diurnal signal.

Simulating synthetic wind power data for a given capacity level then involves “working backwards”. We use a single ARMA model fitted to the noise around the diurnal signal to simulate this residual hourly process over any desired length of time, resulting in a vector called  $U^*$ . To this synthetic time series, the diurnal signals for each calendar month are then re-applied; then synthetic daily means are added, simulated using the twelve ARMA models (**Daily\_ARMA**).

Finally, the resultant hourly time series, which replicates both hourly and daily autocorrelation in historical wind power production, is adjusted to include monthly effects. In order to project the mean and standard deviation of hourly wind energy for each month under much greater levels of installed wind capacity than what exists today, relationships between installed capacity and the mean and standard deviation of hourly wind power production are extrapolated from observed data. For example, the gradual increase of the wind capacity in BPA’s system has led to increased standard deviation of daily wind production (see [Supplementary Information section](#)).

$$\text{Synthetic\_Wind} = (((U^* \times \tilde{\sigma}_h) + \tilde{\mu}_h) \times \text{Log-}\sigma_{m,MW}) + \text{Log-}\mu_{m,MW} \quad (7)$$

where

$\text{Log-}\mu_{m,MW}$  = mean hourly generation in month  $m$ , given capacity MW

$\text{Log-}\sigma_{m,MW}$  = std. deviation of hourly generation in month  $m$ , given capacity MW.

Fig. 4 compares seasonality and hourly autocorrelation for simulated and historical observations. Note that observed wind production (red<sup>1</sup> line) does not have error bars. Since wind capacity

<sup>1</sup> For interpretation of color in Fig. 4, the reader is referred to the web version of this article.

in BPA’s system has grown each year, one representative year (2014) has been selected to test seasonality. Thus this comparison provides a qualitative sense of model accuracy, albeit one that falls a little short of formal validation. It is also important to note that, the synthetic wind energy model performs best in terms of reproducing seasonal effects during the months most important in driving oversupply in the BPA system, i.e., June–August.

### 2.3.5. Daily reservoir operations (modified HYSSR model)

In order to simulate the operations of dams and reservoirs in the BPA system, this study uses a modified version of the Hydro System Seasonal Regulation model (HYSSR), a model designed and built by the US Army Corps of Engineers (USACE). The HYSSR model is a monthly hydro-regulation model that simulates the operation of hydroelectric dams in the Federal Columbia River Power System (FCRPS). It is a deterministic, mass-balance model that produces monthly results for reservoir storage, hydropower production, and reservoir outflow [36]. This model has been used by both BPA and the USACE for planning, operation and regulation purposes (see [Supplemental Information](#) for model schematic).

Since modeling oversupply events requires a time step shorter than monthly, HYSSR has been modified here to a daily model. The modified model includes the operations of 48 dams, which are classified as either storage or run-of-river projects. Storage projects are those that operate based on a set of rules to regulate inflows (i.e., adjust the river’s natural flow pattern to adapt to needs for flood control, water supply, and hydropower production). Storage projects in the FCRPS typically capture peak runoff from spring and summer snowmelt and store it for late summer and autumn release when the natural stream flows are lower. Run-of-river projects have negligible storage capacity and simply pass inflows through turbines for hydropower generation purposes.

The modified HYSSR model calculates each project’s end-of-day storage content, outflow and power generation based on inflows, minimum/maximum discharge requirements, current storage level (only applicable for storage projects) and operational rule curves.

Operational rule curves are determined based on projected inflows, flood control requirements, power generation require-

ments, and a dam's design limitations (e.g., maximum turbine capacity) and regulatory constraints (e.g., minimum environmental flows, minimum elevation for recreation). Using inputs of synthetic unregulated streamflow and reservoir rule curves, the modified HYSSR model yields daily values for reservoir storage and outflow and available hydropower production. It is important to note that not all of the dams in BPA system are represented in HYSSR, but the remaining dams only account for about 12.5% of the total hydropower capacity in this region (see the complete dam list and model schematic in [Supplemental Information](#)). One key assumption made is that the un-modelled 12.5% of hydropower capacity produces electricity proportionally to that produced by dams in HYSSR.

### 2.3.6. Transmission exports

Currently, the maximum export capacity for the BPA system is 13,000 MW. Electricity exports are a function of the availability of surplus power in the BPA system, demand in systems outside BPA, as well as transmission capacity allocation and scheduling. Explicitly modeling transmission exports as a function of all these dynamics is outside of the scope of this current study, but is something that will be addressed in future work.

This study uses a simplifying assumption that BPA used in its own preliminary oversupply analysis [23]. Each hour of the day is classified as either a “high load” hour (6 am–10 pm) or a “low load” hour (11 pm–5 am). A fixed percentage of transmission usage is then assumed for high (90%) and low (70%) load hours, respectively.

### 2.3.7. Hourly system scheduling

A rolling 7-day planning horizon is used when scheduling hourly generation. This builds in flexibility on the part of system operators in scheduling resources to minimize spill at dams, but it also constrains their ability to incorporate future information in dam operations beyond one week.

Due to the specific focus of this study on oversupply events in hydropower-dominated systems, the operations of individual power plants are not modelled via a traditional unit commitment program [16,17]. Rather, the hourly generation scheduling model takes internal system electricity demand, transmission exports, available hydropower and available thermal generation as inputs, then schedules hourly generation, with model output adhering to the following power balance equation:

$$D + X = H + W + T \quad (8)$$

where

- D = electricity demand
- X = electricity export
- H = hydropower production
- W = wind power production
- T = thermal power production.

During the hourly scheduling process, the default assumption is that all available wind power is dispatched (that is, until oversupply conditions occur). It is also assumed that thermal generation is always available to meet any electricity demand not provided by hydropower and wind. This is an assumption that, generally speaking, reflects how thermal generators are used in the BPA system.

During oversupply periods, the hourly scheduling model displaces hydropower production first, forcing dams to “spill” water without generating electricity. This continues until spill discharge reaches the limits imposed by environmental regulations on dissolved gas concentrations (see [Supplemental Information section](#) for details on modeling dissolved gas concentration as a function of spill discharge). At this point, if electricity supply is still greater

than the quantity (demand + exports), thermal generation must be ramped down [18]. A minimum thermal operating capacity of 100 MW is assumed for the entire BPA; this number is set empirically based on the lowest level observed in data from historical information [18]. As a last resort (i.e., if dams are spilling at maximum rates and thermal generation is ramped to its minimum capacity) wind power is curtailed to maintain a balance between both sides of Eq. (8).

## 3. Results and discussion

### 3.1. Model validation

In order to validate the ability of the integrated modeling framework to accurately simulate the frequency and severity of oversupply events in the BPA system, the model's ability to reproduce historical spilling at dams in the FCRPS is verified.

Historical unregulated streamflow data are used to simulate reservoir releases and available hydropower production. Then concurrent historical records of hourly wind power production, thermal generation and transmission exports are subtracted from observed hourly electricity demand for the BPA system, leaving a single hourly time series of net demand. The hourly scheduling model is used to dispatch hydropower generation to meet this net demand. In instances where available hydropower production, as determined by the modified HYSSR model, is greater than net demand, excess water is assumed to be spilled (released from dams without generating electricity).

Simulated vs. observed spilling at all hydroelectric dams over the period 2005–2007 (the only period for which there are overlapping time series of unregulated flow and grid data) is shown in [Fig. 5](#). The model overestimates spilling somewhat in year 2005, but is fairly accurate in 2006 (a particularly wet year). This suggests the model may be more prone to overestimating the occurrence of oversupply events in moderate or dry years. Compared to a wet year, dry and moderate years may give dam operators more flexibility in exercising their own discretion to minimize oversupply events (e.g., dam operators have more room to draw down the storage level for accommodating occasional high flows), but these decisions are more difficult to model. However, cumulative financial losses of oversupply, which is the focus of this study, are driven overwhelmingly by wet years. Thus, overestimating the frequency of small or moderate oversupply events should not greatly impact calculated financial losses, relative to system drivers like installed wind capacity, electricity prices and transmission export capacity.

The model is validated in terms of projected financial losses from wind curtailment. Under 2012 wind capacity levels, modeling results suggest that wind producers in the BPA system experience an average curtailment of 3% of wind power production per year, with losses occasionally reaching 20% in very wet years ([Fig. 6A](#)). BPA's own preliminary analysis suggests that associated annual oversupply losses, given 2012 installed wind capacity and assuming 2012 electricity prices, are an average of \$12 million with a maximum loss of \$50 million. Results of this study, which are based on the same assumptions but also allow for a broader range of possible wind and hydropower production conditions, suggest that the expected annual oversupply loss is \$15 million with a maximum loss of \$96 million ([Fig. 6B](#)).

The difference between these estimates is likely attributable to a combination of modeling bias (the model overestimates the frequency of small and moderate oversupply events) and modeling scope. The modeling framework suggests significantly greater variance than what BPA has identified in the distribution of possible oversupply losses under 2012, including significantly higher maximum annual losses. This is due to the model's use of expanded

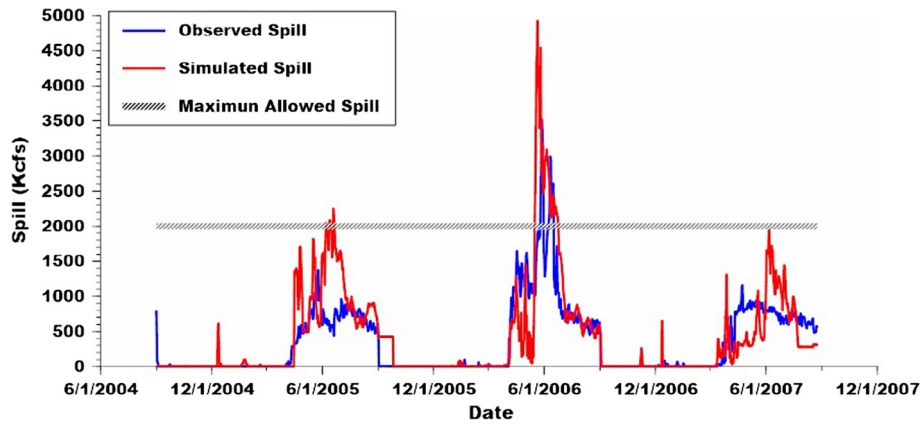


Fig. 5. Spill validation.

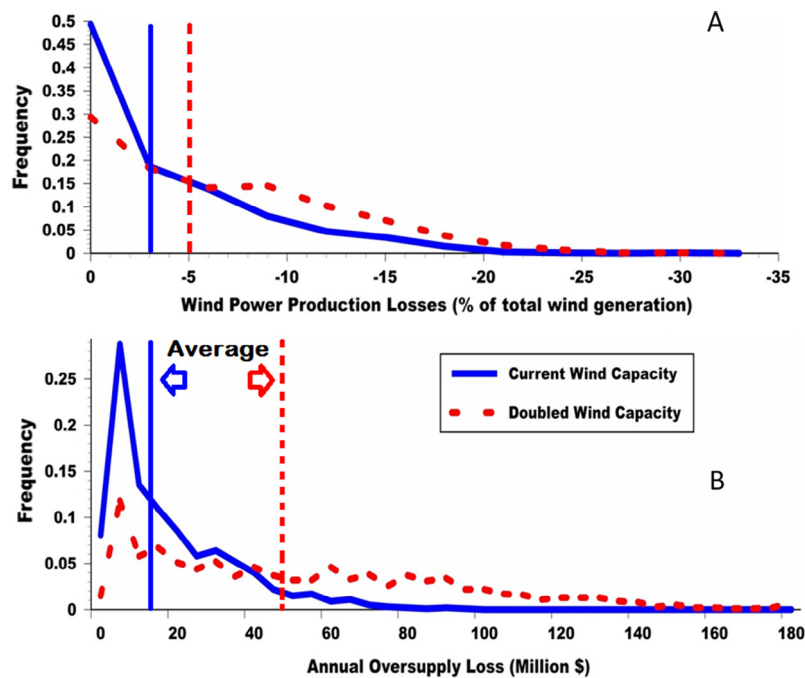


Fig. 6. Distribution of percentage annual wind power production loss (A) & annual oversupply loss in million \$ (B).

synthetic records of streamflows, wind production, and electricity demand, which provide opportunities for the occurrence of values outside the historical record (but within estimated maximum likelihood distributions of each variable).

### 3.2. Sensitivity analysis: double wind capacity

Before evaluating the impacts of a more incremental, long term increase in wind power capacity on oversupply losses, there is also interest in exploring the sensitivity of the BPA system to a doubling of wind power capacity, a condition projected to occur by 2020 [37].

Under this scenario involving doubled wind capacity, average wind curtailment increases to 5% and maximum curtailment rises to 24%. The distribution of financial losses (i.e., the value of curtailed wind power production) under both 2012 and doubled wind power capacity are displayed in Fig. 6A and B. Financial losses are calculated as a combination reduced energy sales and reduced income from renewable energy credits and production tax credits that accrue to wind producers. If wind capacity is doubled, the dis-

tribution of losses shifts to the right and demonstrates much greater variance (a wider “tail”). Annual expected losses grow to \$49 million and the maximum loss estimated to be \$212 million.

### 3.3. Sensitivity analysis: electricity prices

Apart from hydrology and installed wind power capacity, a key driver of financial losses from oversupply events is the price of electricity. The California Independent System Operator (CAISO) is the primary electricity market to which BPA exports excess wind and hydropower [18]. Due to the heavy dependence of California generators on natural gas, wholesale electricity prices in CAISO are strongly correlated with natural gas prices [38]. This is important, because BPA’s initial analysis of oversupply losses assumes 2012 installed wind power capacity and 2012 electricity prices. In fact, natural gas prices were near historic lows in 2012. Although gas prices are projected to remain fairly low for the next several years [39], BPA’s initial estimates of financial losses from oversupply may reflect a fairly unique circumstance involving low electricity prices.

**Table 1**  
Summary of results from sensitivity analysis.

	Modeling scenario	Minimum	Average	Maximum
Curtailment loss	2012 Wind Level	0	3%	20%
	Double 2012 wind level	0	5%	24%
Annual oversupply loss	2012 Wind Level	0	\$15 million	\$96 million
	Double 2012 wind level	0	\$49 million	\$212 million
Electricity price	2012 Price	0	\$15 million	\$96 million
	Recent 10-years	0	\$28 million	\$550 million
	Recent 5-years	0	\$20 million	\$340 million

In order to test the sensitivity of oversupply losses to different electricity prices, expected annual financial losses from oversupply using the 2012 electricity price (\$/MW h) are compared with losses resulting from a wider distribution of electricity prices that incorporates uncertainty in natural gas prices experienced in CAISO over the last 10 years. The results of this comparison suggest that using a wider distribution of electricity prices significantly impacts estimates of the mean annual oversupply loss.

As shown in Table 1, under 10-year price uncertainty, the mean annual oversupply loss increases from about \$15 million to \$28 million, and the maximum oversupply loss dramatically increases to \$550 million (occurring in extremely wet years with very high natural gas prices). However, when only evaluating losses with the most recent 5 years of electricity price data (in which natural gas prices have been low and relatively stable), the mean loss was estimated at \$20 million with a maximum loss of \$340 million.

Overall, this suggests that oversupply losses estimated by BPA using the 2012 electricity price are likely to be underestimates, even if relatively low natural gas prices persist into the future. It is worth noting, however, that a caveat to our sensitivity analysis with regard to price is that we are assuming hydrology and wholesale electricity prices to be independent of one another, when it is known that they generally are correlated in the CAISO market. Although developing a CAISO model is outside of the scope of this study, full analysis of electricity dynamics between BPA and CAISO will be conducted in a future study.

### 3.4. Long term present value losses

The present value (PV) of oversupply losses in the BPA system was also assessed in order to understand these costs from a long term system planning perspective. In particular, there was interest in comparing these losses with the net benefits of expanding transmission capacity in order to export additional excess power and mitigate oversupply losses.

Using an ensemble of 1000 independent 25-year simulations (2016–2040), present value losses were simulated under three different wind capacity growth scenarios, based on BPA projections:

low, mid and high, representing annual growth rates of 300, 400, and 500 MW respectively. Gradual increases in real electricity price were also assumed as projected by EIA, as well as 0.9% annual electricity demand growth. A 4% discount rate was assumed, with all the results presented in 2012 dollars.

In general, the faster wind capacity is added, the greater the PV loss from oversupply events. Results suggest that the low-wind scenario brings about PV losses of between \$273 million to \$883 million over a 25-year period, with a mean of \$529 million. The mid- and high-wind growth scenarios resulted in similar shaped distributions for PV losses (Fig. 7) with minimum PV losses of \$368 million and \$498 million, maximum losses of \$1.06 billion and \$1.25 billion, respectively. The expected 25-year NPV losses for the mid and high wind growth scenarios are \$681 million and \$819 million respectively.

### 3.5. Assessment of transmission expansion as a mitigation strategy

One potential solution for mitigating the impacts of oversupply events is building additional transmission capacity to export excess electricity, in this case to California. This is an option that has been exploited with great success in other systems experiencing oversupply issues, with Texas being the prime example (i.e. ERCOT) [6]. Adding new transmission capacity has also been considered seriously in the BPA system [23].

The impacts of adding transmission capacity on the 25-year present value financial losses from oversupply using mid wind growth are shown in Fig. 8. Results suggest that building a 500 MW transmission line would reduce present value oversupply losses by \$50–60 million over 25 years, whereas building a 1500 MW transmission line would reduce the present value oversupply loss by about \$100–150 million. Although these savings are significant, the cost of building transmission lines is extremely high. On average, building a 500 MW transmission line costs \$1–1.5 million per mile, while 1500 MW transmission lines cost \$2–3 million per mile [40].

In recent years, a 215 mile 1500 MW transmission line was proposed to expand existing connections between BPA and California in order to alleviate future oversupply issues, but this project was

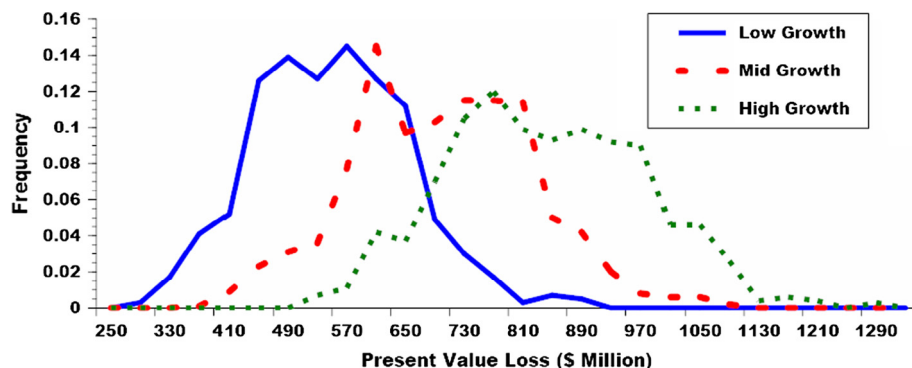


Fig. 7. Present value loss of oversupply losses under different wind growth scenarios over 25 years.

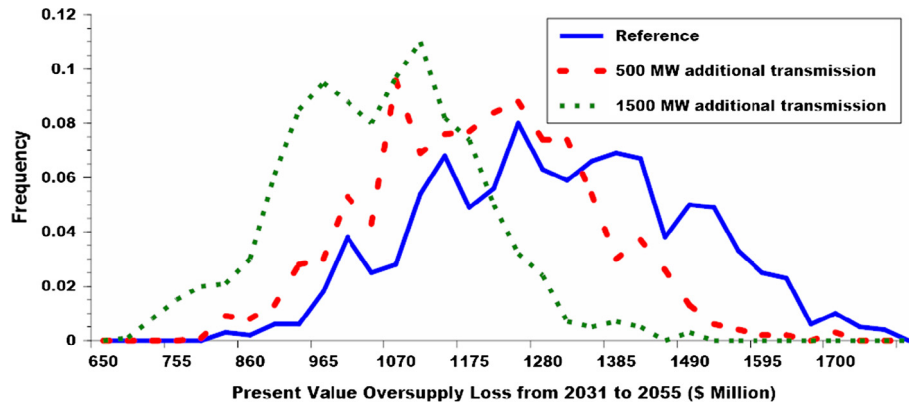


Fig. 8. Impact of transmission upgrades on present value oversupply losses, assuming mid wind growth and transmission upgrade occurs in 2016.

Table 2

Summary of present value losses and the impacts of transmission expansion.

NPV losses	Low wind growth (300 MW)	Mid wind growth (400 MW)	High wind growth (500 MW)
Minimum	\$273 million	\$368 million	\$498 million
Average	\$529 million	\$681 million	\$819 million
Maximum	\$883 million	\$1.06 billion	\$1.25 billion
Transmission expansion	500 MW expansion	1500 MW expansion	
Present value avoided losses (mid wind growth)	\$50–60 million	\$100–150 million	Build year 2016
	\$60–70 million	\$150–200 million	Build year 2030
Expansion cost	\$200–300 million	\$400–600 million	

cancelled in 2015 [41]. The reason for cancellation, according to Portland General Electric (PGE), the developer of this project, had to do with the environmental impacts associated with the proposed transmission line crossing a conservation area. Based on preliminary cost estimates from the Western Electricity Coordinating Council [40], a 215 mile 1500 MW transmission line would cost \$400–600 million. These modeling results suggest that the present value of oversupply losses avoided with the transmission line in place, and assuming gradually increasing 2012 electricity prices, are well below the cost of new transmission capacity even before considering its potential environmental impacts.

It is possible, however, that this transmission project (or one like it) may be reconsidered by BPA in the future, and over time its economic viability may change. The discounting nature of the present value calculation makes larger oversupply losses that are likely to occur out in the future as a result of growing wind capacity less impactful.

Therefore, the viability of the proposed (and now cancelled) transmission line is also assessed for future years (Table 2). Specifically, starting in 2030, the present value of oversupply losses over 25 years (2031–2055) is calculated, with assumptions of continuous growth of wind and steady increases in electricity price (as projected by the EIA). Under these circumstances, the 500 MW transmission upgrade project would reduce the 2030 PV loss by about \$70 million and the 1500 MW project would reduce present value oversupply losses by \$160–210 million. This still falls well short of the cost of developing new transmission capacity, suggesting that such a project is unlikely to be financially attractive in the foreseeable future.

### 3.6. Study limitations and future work

This analysis has several of limitations. Key factors not considered are changes in snowmelt timing and streamflow dynamics that are projected to occur as a result of climate change. The distribution of total annual precipitation may shift, leading to higher or

lower annual total streamflow. The percentage of precipitation falling as rain vs. snow may also change, as well as the timing of snowmelt. All of this would impact the timing and amount of water spilled during high flow events, and the frequency and severity of oversupply [42].

It is also worth mentioning that this work does not include consideration of the dynamic nature of electricity pricing in the CAISO market. This study demonstrates that the wholesale electricity price can have a major impact on both expected and maximum oversupply losses. However, it's important to recognize that oversupply periods alter the wholesale electricity price. Likewise, rules in CAISO for dealing with periods of oversupply are subject to change. Currently, the market allows prices to fall below zero to encourage generators who can ramp down production to do so. However, the current minimum price ( $-\$20/\text{MW h}$ ) does not impose a sufficient financial penalty on wind producers, as the combination of tax credits (REC and PTC) pays more than  $\$20/\text{MW h}$ . In recent years, CAISO has considered lowering the negative floor to  $-\$1000/\text{MW h}$  [23], a change that could impose significantly greater financial penalties on BPA and its customers when oversupply occurs.

## 4. Conclusions

As variable renewable energy capacity grows, the potential for oversupply events and regular curtailment of these sources may present increasing challenges. Oversupply is occurring with greater frequency in the hydropower-dominated Pacific Northwest region of the U.S., where wind energy curtailment is common during wet years when hydropower is plentiful.

With respect to the BPA system in particular, results suggest that continued growth of wind power capacity could lead to higher oversupply-related financial losses in the future. However, these results are sensitive to assumptions about the wholesale electricity price. Results also suggest that, while additional transmission capacity could mitigate a significant portion of oversupply-

related losses in the BPA system, these avoided losses are unlikely to justify the substantial cost of developing this infrastructure. Consequently, curtailment of wind power during oversupply conditions appears to be a more cost effective solution than new transmission capacity, at least for the foreseeable future.

Given expectations of continued growth in renewable energy capacity, renewable curtailment is expected to happen more often while imposing ever larger financial losses. Despite the associated energy waste and financial losses, these results suggest that curtailment can be considered a practical short- to medium-term solution to manage electrical grid stability in the face of oversupply in settings such as BPA. However, this study does not consider other economic benefits of building transmission infrastructure, such as the potential for reduced carbon emissions and reduced fuel costs in thermal dominated systems. In many thermal dominated regions in the U.S., systems are actively building additional transmission lines to help incorporate greater renewable integration partially because of these additional economic values.

This study demonstrates that a hydro-economic systems model can be used to characterize the physical (spilling, wind curtailment) and financial consequences of oversupply events. It also demonstrates the utility of our modeling framework in providing long term system planning insights under uncertainty, particularly with respect to installed wind capacity and electricity prices. From a general perspective, this modeling approach can provide a foundation for developing strategies that mitigate a renewable generator's financial risk or be used by planners to make more informed decisions on future infrastructure investments, such as expanded transmission capacity. The methodology and analysis presented in this work can also be used to gain insights on a host of other critical issues, particularly if it is expanded to capture complex and convoluted interactions with neighboring systems.

## Acknowledgements

This work was funded by the UNC-Chapel Hill Institute of the Environment.

## Appendix A. Supplementary material

Supplementary data associated with this article can be found, in the online version, at <http://dx.doi.org/10.1016/j.apenergy.2017.02.067>.

## References

- [1] GWEC. Global wind statistics 2015; 2016.
- [2] Bélanger C, Gagnon L. Adding wind energy to hydropower. *Energy Policy* 2002;30(14):1279–84. Available at: <http://www.sciencedirect.com/science/article/pii/S0301421502000897>.
- [3] De Jonghe C, Delarue E, Relmans R, D'haeseller W. Determining optimal electricity technology mix with high level of wind power penetration. *Appl Energy* 2011;88(6):2231–8. <http://dx.doi.org/10.1016/j.apenergy.2010.12.046>.
- [4] NREL. Integration of wind and hydropower systems - volume 1: issues, impacts and economics of wind and hydropower generation. 1; 2011.
- [5] Jaramillo OA, Borja MA, Huacuz JM. Using hydropower to complement wind energy: a hybrid system to provide firm power. *Renewable Energy* 2004;29(11):1887–909. Available at: <http://linkinghub.elsevier.com/retrieve/pii/S0960148104000928>.
- [6] Lew D, Bird L, Milligan M, Yoh Y. Wind and solar curtailment preprint. In: International workshop on large-scale integration of wind power into power systems, (September); 2013. Available at: <http://citeseerx.ist.psu.edu/viewdoc/download?doi=10.1.1.390.1983&rep=rep1&type=pdf>.
- [7] Olson Arne, Jones Ryan A, Hart Elaine, Hargreaves Jeremy. Renewable curtailment as a power system flexibility resource. *Electr J* 2014;27(9):49–61. <http://dx.doi.org/10.1016/j.tej.2014.10.005>.
- [8] Li C, Shi H, Cao Y, Wang J, Kuang Y, Tan Y, et al. Comprehensive review of renewable energy curtailment and avoidance: a specific example in China. *Renew Sustain Energy Rev* 2015;41:1067–79. Available at: <http://www.sciencedirect.com/science/article/pii/S1364032114007825>.
- [9] Bird L, Cochran J, Wang X. Wind and solar energy curtailment: experience and practices in the United States; 2014 (March). p. 51. Available at: <http://www.nrel.gov/docs/fy14osti/60983.pdf>.
- [10] Klinge Jacobsen H, Schröder ST. Curtailment of renewable generation: Economic optimality and incentives. *Energy Policy* 2012;49C:663–75.
- [11] Denholm P. Energy storage to reduce renewable energy curtailment. 2012 IEEE Power and Energy Society General Meeting, San Diego, CA; 2012. p. 1–4.
- [12] Foley AM, Leahy PG, Li K, McKeogh EJ, Morrison AP. A long-term analysis of pumped hydro storage to firm wind power. *Appl Energy* 2015;137:638–48.
- [13] Hirth L. The benefits of flexibility: the value of wind energy with hydropower. *Appl Energy* 2016;181:210–23. Available at: <http://linkinghub.elsevier.com/retrieve/pii/S0306261916309801>.
- [14] Wisner Ryan, Bolinger Mark, Heath Garvin, Keyser David, Lantz Eric, Macknick Jordan, et al. Long-term implications of sustained wind power growth in the United States: potential benefits and secondary impacts. *Appl Energy* 2016;179:146–58. <http://dx.doi.org/10.1016/j.apenergy.2016.07.023>.
- [15] Zhang N, Lu X, McElroy MB, Nielsen CP, Chen X, Deng Y, et al. Reducing curtailment of wind electricity in China by employing electric boilers for heat and pumped hydro for energy storage. *Appl Energy* 2016;184:987–94. Available at: <http://www.sciencedirect.com/science/article/pii/S0306261915013896>.
- [16] Kern JD, Patino-Echeverri D, Characklis GW. An integrated reservoir-power system model for evaluating the impacts of wind integration on hydropower resources. *Renewable Energy* 2014;71:553–62. <http://dx.doi.org/10.1016/j.renene.2014.06.014>.
- [17] Kern JD, Patino-Echeverri D, Characklis GW. The impacts of wind power integration on sub-daily variation in river flows downstream of hydroelectric dams. *Environ Sci Technol* 2014;48(16):9844–51. Available at: <http://pubs.acs.org/doi/abs/10.1021/es405437h%5Cnhttp://www.ncbi.nlm.nih.gov/pubmed/25061693>.
- [18] BPA. 2015 BPA facts; 2015.
- [19] EIA.gov. BPA curtails wind power generators during high hydropower conditions; 2011. Available at: <http://www.eia.gov/todayinenergy/detail.cfm?id=1810>.
- [20] BPA. Working together to address Northwest oversupply of power; 2012. Available at: <https://www.bpa.gov/Projects/Initiatives/Oversupply/OversupplyDocuments/EnvironmentalRedispatch-WorkingTogether-May2011.pdf>.
- [21] Bonneville Power Administration & Corps, A. BPA and Fish Passage Center study effects of changing total dissolved gas standards April 2011; 2011 (April). p. 1–3. Available at: [https://www.bpa.gov/Projects/Initiatives/Oversupply/OversupplyDocuments/TDG\\_Analysis\\_APR\\_2011.pdf](https://www.bpa.gov/Projects/Initiatives/Oversupply/OversupplyDocuments/TDG_Analysis_APR_2011.pdf).
- [22] Sale MJ. Reduced spill at hydropower dams: opportunities for more generation and increased fish protection; 2006.
- [23] Bonneville Power Administration. Northwest overgeneration: an assessment of potential magnitude and cost; 2013. p. 1–14. Available at: [http://www.bpa.gov/Projects/Initiatives/Oversupply/OversupplyDocuments/BPA\\_Overgeneration\\_Analysis.pdf](http://www.bpa.gov/Projects/Initiatives/Oversupply/OversupplyDocuments/BPA_Overgeneration_Analysis.pdf).
- [24] Peter B. Bonneville power to wind generators – shut down, and you get free power. *The New York Times*; 2011. Available at: <http://www.nytimes.com/cwire/2011/02/25/25climatewire-bonneville-power-to-wind-generators-shut-dow-22723.html?pagewanted=all>.
- [25] BPA. About BPA. Available at: <https://www.bpa.gov/news/AboutUs/Pages/default.aspx> [accessed December 6, 2016].
- [26] BPA. 2010 modified streamflow; 2010. Available at: <https://www.bpa.gov/power/streamflow/default.aspx> [accessed October 7, 2015].
- [27] National Oceanic and Atmospheric Administration (NOAA) temperature datasets; 2015. Available at: <https://www.ncdc.noaa.gov/cdo-web/datatools/findstation> [accessed October 6, 2015].
- [28] Nowak K, Prairie J, Rajagopalan B, Lall U. A nonparametric stochastic approach for multisite disaggregation of annual to daily streamflow. *Water Resour Res* 2010;46(8).
- [29] Nawaz S, Iqbal N, Anwar S. Modelling electricity demand using the STAR (smooth transition auto-regressive) model in Pakistan. *Energy* 2014;78:535–42. <http://dx.doi.org/10.1016/j.energy.2014.10.040>.
- [30] Engle RF, Mustafa C, Rice J. Modeling peak electricity demand. *J Forecasting* 1992;11(3):241–51. Available at: <http://onlinelibrary.wiley.com/doi/10.1002/for.3980110306/abstract>.
- [31] The Northwest Power and Conservation Council. Electricity demand forecast. In: Seventh northwest conservation and electric power plan; 2015. Available at: [https://www.nwcouncil.org/media/7149931/7thplanfinal\\_chap07\\_demandforecast.pdf](https://www.nwcouncil.org/media/7149931/7thplanfinal_chap07_demandforecast.pdf).
- [32] Billinton R, Chen HUA. Time series models for reliability evaluation of power systems including wind energy. *Microelectron Reliab* 1996;36(9):1253–61.
- [33] Castino F, Festa R, Ratto CF. Stochastic modelling of wind velocities time series. *J Wind Eng Ind Aerodyn* 1998;74–76:141–51.
- [34] Morgan Eugene C, Lackner Matthew, Vogel Richard M, Baise Laurie G. Probability distributions for offshore wind speeds. *Energy Convers Manage* 2011;52(1):15–26. <http://dx.doi.org/10.1016/j.enconman.2010.06.015>.
- [35] Papavasiliou A, Oren SS. Stochastic modeling of multi-area wind power production; 2012.
- [36] USACE. Models used in power and operations planning at BPA compiled by Tony White. Spring 2008 for the RMJOCIE; 2008.
- [37] BPA Wind Generation & Total load in the BPA; 2014. Available at: <https://transmission.bpa.gov/business/operations/wind/> [accessed December 2, 2015].

- [38] Woo CK, Moore J, Schneiderman B, Ho T, Olson A, Alagappan L, et al. Merit-order effects of renewable energy and price divergence in California's day-ahead and real-time electricity markets. *Energy Policy* 2016;92:299–312.
- [39] EIA. Annual energy outlook 2016 Available at: <http://www.eia.gov/forecasts/aeo/>; 2016.
- [40] Pletka R, Khangura J, Rawlins A, Waldren E, Wilson D. Capital costs for transmission and substations. Western Electricity Coordinating Council; 2014 (February). p. 35.
- [41] PGE, BOA Cancel Plans for Major Transmission Line; 2015. Available at: <http://www.opb.org/news/article/pge-bpa-cancel-plans-for-major-transmission-line/> [accessed April 2, 2016].
- [42] U.S. Army Corps of Engineers, P.D. & (BPA) Bonneville Power Administration. Draft climate and hydrology datasets for use in the RMJOC agencies' longer-term planning studies Part III - reservoir operations assessment. Columbia Basin Flood Control and Hydropower; 2011.